

# An Improved Networked Predictive Controller for Vascular Robot Using 5G Networks

Lin-Sen Zhang<sup>1,2</sup>, Shi-Qi Liu<sup>2</sup>, Xiao-Liang Xie<sup>2</sup>, Xiao-Hu Zhou<sup>2</sup>, Zeng-Guang Hou<sup>2,3</sup>,  
Yan-Jie Zhou<sup>2</sup>, Han-Lin Zhao<sup>2</sup>, and Mei-Jiang Gui<sup>2</sup>

**Abstract**—Percutaneous coronary intervention (PCI) has gradually become the most common treatment of coronary artery disease (CAD) in clinical practice due to its advantages of small trauma and quick recovery. However, the availability of hospitals with cardiac catheterization facilities and trained interventionalists is extremely limited in remote and underdeveloped areas. Remote vascular robotic system can assist interventionalists to complete operations precisely, and reduce occupational health hazards occurrence. In this paper, a bionic remote vascular robot is introduced in detail from three parts: mechanism, communication architecture, and controller model. Firstly, human finger-like mechanisms in vascular robot enable the interventionalists to advance, retract and rotate the guidewires or balloons. Secondly, a 5G-based communication system is built to satisfy the end-to-end requirements of strong data transmission and packet priority setting in remote robot control. Thirdly, a generalized predictive controller (GPC) is developed to suppress the effect of time-varying network delay and parameter identification error, while adding a designed polynomial compensation module to reduce tracking error and improve system responsiveness. Then, the simulation experiment verifies the system performance in comparison with different algorithms, network delay, and packet loss rate. Finally, the improved control system conducted PCI on an experimental pig, which reduced the delivery integral absolute error (IAE) by at least 20% compared with traditional methods.

## I. INTRODUCTION

Cardiovascular disease is currently the greatest threat to human health in the world. Vascular interventional surgery has been gradually conducted to cure cardiovascular and cerebrovascular diseases due to its advantages of smaller incisions and quicker recovery. However, X-ray exposure under fluoroscopically guided interventional procedures and heavyweight of interventional suites may predispose interventionalists to distinct occupational health hazards [1].

Compared with manual delivery by interventional radiologists, the vascular robot has the advantages of safety,

\*This work was supported in part by the National Key Research and Development Program of China under Grant 2019YFB1311700; in part by the National Natural Science Foundation of China under Grant 62073325, Grant 62003343, and Grant U20A20224; in part by the Youth Innovation Promotion Association of CAS under Grant 2020140; and in part by the Strategic Priority Research Program of CAS under Grant XDB32040000.

<sup>1</sup>University of Science and Technology Beijing, Beijing 100083, China; Email:zhanglinsen@aliyun.com

<sup>2</sup>State Key Laboratory of Management and Control for Complex Systems, Institute of Automation, Chinese Academy of Sciences, Beijing 100190, China.

<sup>3</sup>CAS Center for Excellence in Brain Science and Intelligence Technology, Beijing 100190, China, and also with CASIA-MUST Joint Laboratory of Intelligence Science and Technology, Institute of Systems Engineering, Macau University of Science and Technology, China; Email:zengguang.hou@ia.ac.cn

efficiency, and accuracy. After the vascular robot is connected to the Internet, interventional radiologists can perform operations on patients in areas with poor medical conditions, reducing the risk of delayed treatment due to referrals. Telemedicine recently has achieved great success in the field of orthopedic surgery and will continue to expand [2], [3].

In the past, 4G networks do not have enough bandwidth to send massive data packets, nor does it have low-latency services [4]. 5G networks using network slicing and time-sensitive networking (TSN) can communicate with ultra-low delay under the condition of large throughput, which means that robots can transmit more sensor signals and video signals in real-time to improve control transparency [5], [6].

Network Predictive Control (NPC) is a combination of networked control systems (NCSs) and predictive control. For NCSs, dynamic random delay and packet loss will greatly reduce the control stability and system performance [7]. The wave variable control is based on the passivity principle, by converting control signals into energy signals, to ensure internal energy conservation and system stability [8]. However, the delay-jitter will cause the system shock because the energy wave cannot be depleted in time. Smith predictive control can assure the system stability under constant time delay, but it needs to obtain the precise system model [9]. The dynamic scheduling method dynamically changes the sampling period and control gain of the system, which will deteriorate the transient performance of the system [10]. GPC periodically identifies system models through the past input and output signals, which can ensure stability and dynamic performance under the model parameter perturbation and external disturbance [11]. However, the output phase lag caused by the network delay cannot be resolved, which will affect the tracking performance of the system and reduce the transparency of the doctors' teleoperation.

In the remaining parts of this study, Section II describes a master-slave vascular robot, including mechanical structure, control architecture, and network communication model. Section III describes an improved network controller based on GPC to control the slave robot under the dynamic random delay and bounded packet loss network. Then the simulation and animal experimental results are presented in Section IV, and Section V concludes the paper.

## II. SYSTEM FRAMEWORK

### A. Mechanism

In actual surgery, interventional radiologists use two fingers to push and twist guidewires or catheters to complete

longitudinal and axial operations. Based on the bionic heuristic mechanism, the master-slave vascular robot uses two rollers to imitate these movements by rotating back and forth or moving relative to each other longitudinally. A DC motor is installed under the middle rollers as a driving wheel (yellow wheel), and other rollers are driven wheels, which can control the guidewire forward and backward. A lifting device is respectively installed under the two driven wheels, which can control the guidewire to rotate clockwise or counterclockwise. A wheelbase adjusting device is arranged under the driven wheel (white wheels), and the clamping or releasing of the roller is controlled by adjusting the wheelbase. The outsides of rollers are wrapped with rings of rubber, which can increase the friction on the guidewire and the catheter. All motors are equipped with reduction gearboxes to increase output torque and operation accuracy.

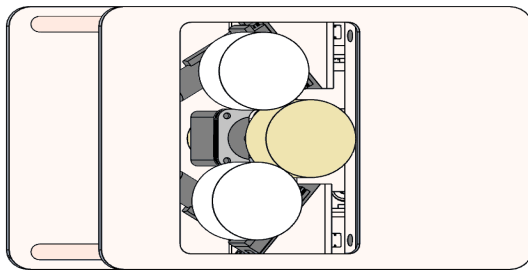


Fig. 1. Multi-instrument collaborative remote vascular robot 3D diagram

### B. Network Communication Model

There are four main types of communication signals in the network model, including main setting, clock sync, time base, and control signals. According to signals priorities of timeliness and integrity, they are sent using different protocols. Owing to asymmetry of the network, the uplink latency ( $\tau_{s2m}$ ) and downlink latency ( $\tau_{m2s}$ ) may not be equal. IEEE1588 PTP (Precision Time Protocol) based on the four-way handshake is used to synchronize the local clocks at both ends [12]. After two local clocks are synchronized, the uplink and downlink delays can be calculated separately according to data packets' timestamps. Quality of service (QoS) indicators such as packet loss rate and bandwidth are approximated by some algorithms, which are used to assess network quality to alarm when the network is in a bad state.

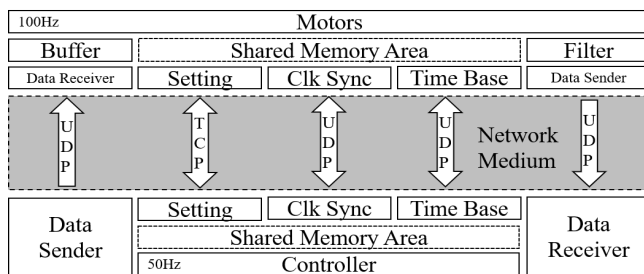


Fig. 2. Structure diagram of communication system under network control

### C. Control Architecture

Each motor (Maxon 118777) is driven by a servo controller (Maxon). Encoders with a resolution of 500 pulses per revolution are installed at the rear of the motors for angle detection. The whole control system has two main tasks, one is to collect the sensor signals and DSA images from the slave robot, and the other is to send doctors' input signals to the slave controller (STM32H7) after being processed by the master controller (STM32H7). The motor control signals are converted to PWM (Pulse Width Modulation) signals on the motor drive board to control DC motors. At the same time, the slave controller collects sensor data and returns it to the master after preprocessing to complete the closed-loop.

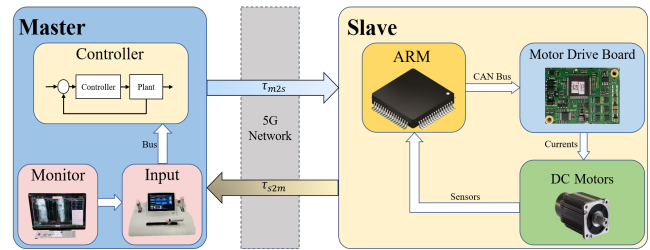


Fig. 3. Master-slave remote control structure diagram under 5G network

## III. CONTROLLER DESIGN

The networked predictive controllers in vascular robot have two functions, one is to improve the tracking performance under varying delay, and the other is to enhance the robustness of the system under bounded packet loss. For bounded packet loss compensation, probability constraints are used to reduce empty sampling caused by packet loss by increasing the frequency of data packet transmission [13], [14]. The following introduces the improved GPC controller in our vascular robotic system.

### A. Generalized Predictive Control

GPC is a type of model predictive control (MPC). It is a combination of adaptive control and predictive control. Given the model uncertainty caused by the dynamic random network latency, GPC can be used to periodically adjust the controller parameters without knowing the precise model, which can be identified in real-time according to past input and past output signals. Compared with MPC, the CARIMA (Controlled Auto-Regressive Integrated Moving Average) model of GPC is more suitable for discrete systems with hysteresis, and the single-step operation requires less calculation [15].

The CARIMA model of GPC is:

$$(1 - z^{-1})A(z^{-1})y(k) = B(z^{-1})\Delta u(k-1) + c(z^{-1})\xi(k) \quad (1)$$

where  $A$ ,  $B$ , and  $C$  (constant value) are discrete parameter equations which represent the inherent performance of the system,  $\Delta u$  is the incremental form of the control increment, and  $\xi$  is the white noise sequence (simulating the disturbance).  $k$  is the number of beats of control system.  $z^{-1}$  represents the complex variable operator.

Select the performance index function as follows:

$$J = E\{[Y(k+j) - Y_r(k+j)]^T Q[Y(k+j) - Y_r(k+j)] + \Delta U^T(k) R \Delta U(k)\} \quad (2)$$

where  $Y(k+j)$  is the predictive future output in predict horizon,  $Y_r(k+j)$  is the expected future output vector,  $\Delta U(k)$  is the current and future control increment vector in control horizon,  $Q$  and  $R$  are the weighting matrixes.

Under the constraint of  $J$ , the system can minimize the output error under the least control quantity. After the iterative calculations of the diophantine equation, the final output vector can be obtained as shown below:

$$Y(k+j) = L\Delta U(k) + H\Delta U(k-j) + GY(k) + E\xi(k+j) \quad (3)$$

where  $\Delta U(k-j)$  is past control increment vector, and  $\Delta Y(k)$  is past output vector.

It can be seen from the equation that the system outputs at the current and future moments are related to the past output vector and the past control vector. Incorporating Equation (3) into Equation (2), the control increment of the  $k$ th beat can be obtained as shown below from  $\partial J / \partial \Delta U(k) = 0$ :

$$\Delta u(k) = d_1^T [Y_r(k+j) - H\Delta U(k-j) - GY(k)] \quad (4)$$

where matrix  $H$  and  $G$  are diophantine matrices, which can be calculated through system equations defined by  $A$ ,  $B$  in Equation (1).  $d_1$  is the first row of the matrix.

Changes in communication delay cause model parameter perturbation. The least-square method with forgetting factor is used to estimate the system.

$$\begin{aligned} \hat{\theta}(k) &= \hat{\theta}(k-1) + K(k)[\Delta y(k) - \varphi^T(k)\hat{\theta}(k-1)] \\ K(k) &= \frac{P(k-1)\varphi(k)}{\lambda + \varphi^T(k)P(k-1)\varphi(k)} \\ P(k) &= \frac{1}{\lambda} [I - K(k)\varphi^T(k)]P(k-1) \end{aligned} \quad (5)$$

where  $\theta$  contains all identified parameters of the system equations  $A$  and  $B$ , and  $\varphi$  contains the value of output increment and control increment in the last predict horizon.

### B. Polynomial Predictive Controller

The GPC controller above can ensure the stability of the system under the feedback delay after tests. However, since the expected future output vector  $Y_r$  is only related to the current input value. There will always be a phase lag between the system output and the input because of  $\tau_{m2s}$  delay. So we designed an advanced trajectory generation module based on a polynomial fitter to compensate for the phase lag.

$$\begin{bmatrix} Y_r(k-N) \\ Y_r(k-N+1) \\ \vdots \\ Y_r(k) \end{bmatrix} = \begin{bmatrix} (k-N)^0 & \cdots & (k-N)^M \\ (k-N+1)^0 & \cdots & (k-N+1)^M \\ \vdots & \ddots & \vdots \\ k^0 & \cdots & k^M \end{bmatrix} \begin{bmatrix} c_0 \\ c_1 \\ \vdots \\ c_M \end{bmatrix} \quad (6)$$

The polynomial equation form of the output is shown in Equation (6), where  $N$  is the number of fitting elements,  $M$  is the polynomial order, and  $c$  are the polynomial coefficients.

$$Y_r^*(k) = Y_r(k+d) = C_0 + C_1(k+d) + \dots + C_M(k+d)^M \quad (7)$$

where  $d$  is the delayed beats of  $\tau_{m2s}$ . Through the polynomial fitter, the trajectory is corrected to be ahead of the input signal trajectory by  $d$  beats to reduce tracking error.

$$Y_r(k+d) = \begin{cases} Y_r^*(k) & \Delta Y_r \neq 0, \Delta Y_r' \neq 0, k \geq N \\ Y_r^*(k) & \Delta Y_r \neq 0, \Delta Y_r' = 0, k \geq N \\ Y_r(k) & \Delta Y_r = 0, \Delta Y_r' = 0, k \geq N \\ Y_r(k) & k < N \end{cases} \quad (8)$$

By analyzing the historical input signals of the doctor operating the robot, we classify the signals into the above three types, which are simulated with sine, sigmoid, parabola, slope, and step signals. To prevent the system from oscillating, the input signal of the compensator has been low-pass filtered. These five signals include uniform motion, uniformly variable motion, and variable acceleration motion, which approximately cover all types of doctor input signals.

## IV. EXPERIMENTS

### A. Simulation

The tracking performance of different control methods is compared on the simulation platform. In the experiment, the time delay module is used to simulate the communication latency. The delay signal consists of a fixed delay and a square wave jitter delay, with an average value of 120ms. Compare the tracking performance of different control methods under sinusoidal signal input when the system model is a first-order inertial system.

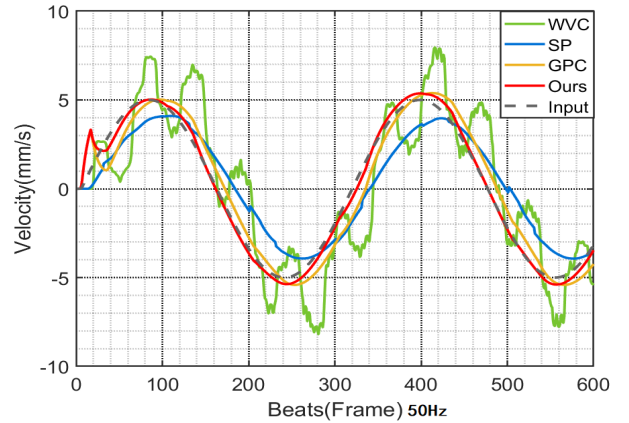


Fig. 4. Comparison of the tracking performance of three control algorithms under random delay jitter. The black line represents the input signal, WVC represents the wave variable control, SP represents the smith predict control, the yellow line represents the GPC, and the red line represents our controller.

The simulation experiment verifies that the GPC controller can ensure stable control under system model parameter perturbation caused by communication delay, but there is a problem of output signal phase lag. The smith control and

TABLE I  
COMPARISON OF IAE IN ANIMAL EXPERIMENTS UNDER DIFFERENT SYSTEM STRUCTURES AND VELOCITIES

Method	Sine			Slope			Step			Sigmoid			Parabola		
	10	20	100	10	20	100	10	20	100	10	20	100	10	20	100
GPC only	416	1550	4592	376	261	2504	122	200	554	261	251	1024	372	249	1246
ours,rank=1	408	910	3335	300	220	1868	<b>112</b>	<b>195</b>	<b>516</b>	256	222	976	265	162	820
ours,rank=3	<b>240</b>	<b>478</b>	<b>1999</b>	<b>294</b>	<b>188</b>	<b>1824</b>	113	199	560	255	<b>202</b>	758	229	207	740
ours,rank=5	261	733	4048	368	240	2379	<b>112</b>	210	540	<b>208</b>	209	<b>760</b>	<b>217</b>	<b>150</b>	<b>736</b>

wave variable control causes system oscillations and even instability. The system after adding a polynomial compensator can effectively improve the lag caused by network delay and improve signal tracking performance.

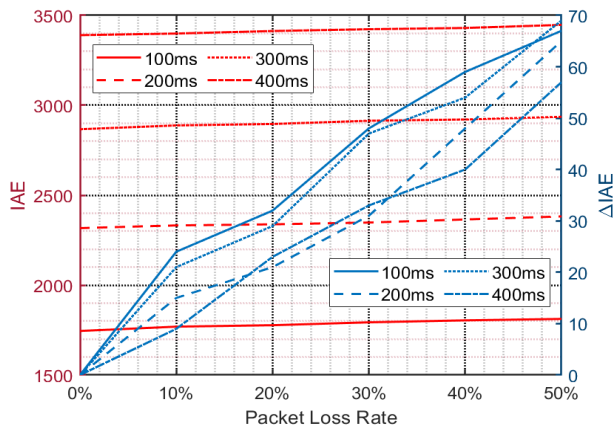


Fig. 5. Comparison of IAE in GPC under different delay and packet loss rate from sinusoidal signal input. The red lines represent the comparison of the absolute value of IAE, and the coordinate axis is on the left; the blue lines represent the incremental value of IAE, and the coordinate axis is on the right.

The simulation experiment also carried out a comparison of the tracking performance of the system under different packet loss rates. The system uses a switch module and memory module to simulate packet loss under real communication conditions. The experiment tested the impact of different packet loss rates on the tracking performance of the system from 100ms to 400ms. As shown in the figure above, the tracking performance of the system decreases approximately linearly with the continuous increase of the packet loss rate, but compared with the increase of the packet loss rate, the increase in network delay has a greater impact on the tracking error. Therefore, the GPC controller and probability constraints compensator were added to solve the delay and packet loss problems respectively.

### B. Remote Live Animal Experiment

The experimental locations were Beijing and Shanghai (over 1000km); one of the master controllers was deployed in the laboratory (Beijing); the slave robot was deployed in the operating room of the Huadong Hospital affiliated to Fudan University (Shanghai). The master and slave communicated through 5G networks provided by two 5G CPEs (Customer

Premise Equipment). The average round-trip time throughout the experiment was 120ms, and the average packet loss rate was 5%. The animal experiment subject is an anesthetized live Bama minipig (30kg weight), and the experiment tasks are the delivery of the guidewire in the coronary artery. This study had been approved by The Experimental Animal Ethics Committee. After placing the catheter in the coronary artery of the experimental pig, a remote animal guidewire delivery experiment was performed. Experiments have tested different velocities, compensator structures, and signal types to evaluate the performance of the control system during the actual operation. In the experiment, the guidewire is delivered from the initial position of the catheter port to the position where the single task cycle ended, and the program controls the guidewire to return to the initial position after the end of a single experiment. Each group of experiments was carried out five times, and the data were averaged.

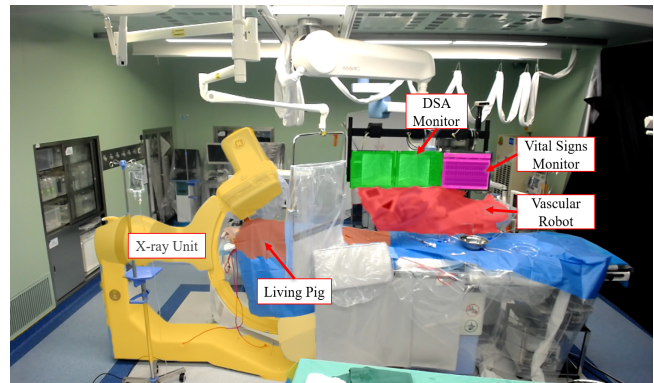


Fig. 6. Remote PCI experiment on the experimental pig

### C. Results and Discussion

The experiment compared the IAE under the control of the single GPC controller and the improved controller, and both systems ensured stability during the experiment. The system after adding the polynomial compensator reduces IAE in most cases. The tracking performance has achieved a better improvement effect on signals with frequent changes in acceleration. The third-order and fifth-order compensators have the best optimization results in this experiment. As the input signal amplitude increases, the IAE optimization rate also increases. At three typical speeds, the improved system can reduce IAE by an average of 20%, which improves

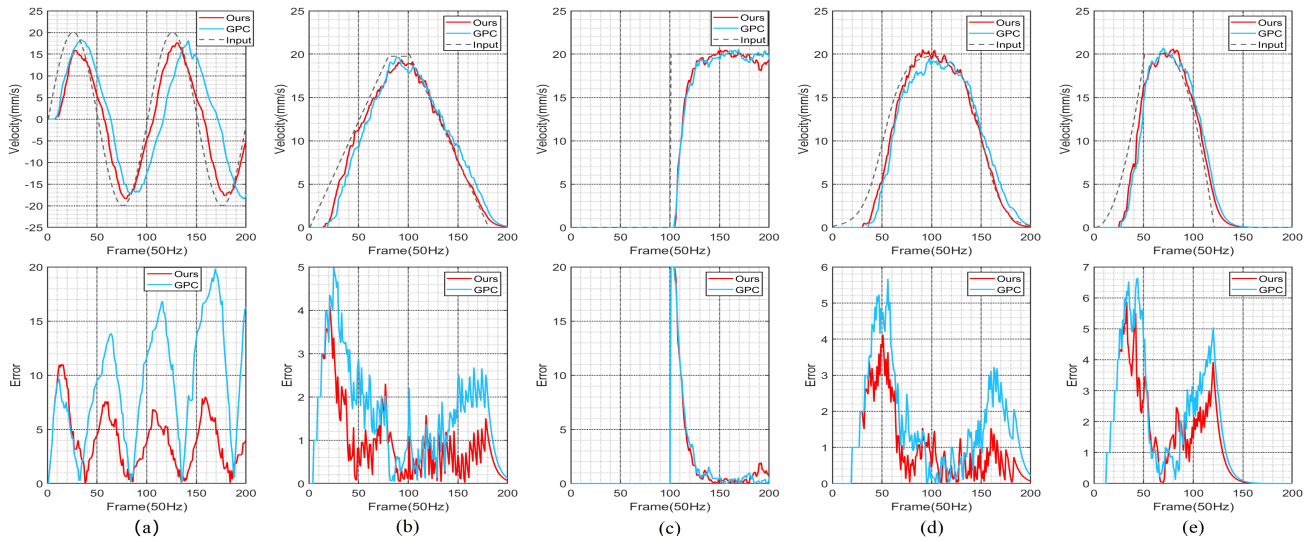


Fig. 7. The data comparison chart under five signal inputs in animal experiments. Diagrams (a), (b), (c), (d), and (e) respectively represent the system output and error diagrams under sine input, ramp input, step input, sigmoid input, and parabolic input. The blue line is the curve of the traditional GPC controller, and the red line is the curve of the improved system after adding a compensator.

tracking performance without decreasing system stability. It should be pointed out that in the experiment, the guidewire deformation, tip collision may affect the accuracy of the results.

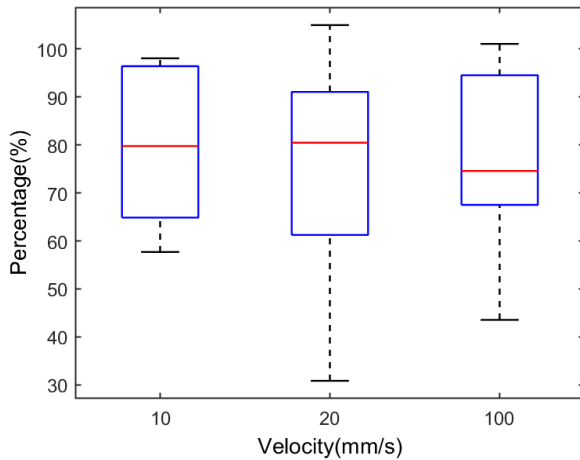


Fig. 8. The IAE optimization rate of the improved control system compared to single GPC control system at different speeds

## V. CONCLUSIONS

This paper presents the detailed design of a master-slave networked control vascular robot, including the mechanical structure, network communication model, and control system design. The experimental results confirm that the networked control system of the vascular robot has better robustness and better tracking performance in remote surgery. The control performances of the robotic system can be further improved to better match the medical demands by introducing other optimization methods.

## REFERENCES

- [1] L. W. Klein, et al, "Occupational health hazards in the interventional laboratory: time for a safer environment," *Radiology*, vol. 250, no. 2, pp. 538-544, 2009.
- [2] W. Tian, et al, "Telerobotic spinal surgery based on 5G network: the first 12 cases," *Neurospine*, vol. 17, no. 1, p. 114, 2020.
- [3] G. Aceto, et al, "Industry 4.0 and health: internet of things, big data, and cloud computing for healthcare 4.0," *Journal of Industrial Information Integration*, vol. 18, p. 100129, 2020.
- [4] E. Hajlaoui, et al, "4G and 5G technologies: a comparative study," in *Proceedings of International Conference on Advanced Technologies for Signal and Image Processing*, pp. 1-6, 2020.
- [5] I. Afolabi, et al, "Network slicing and softwarization: a survey on principles, enabling technologies, and solutions," *IEEE Communications Surveys & Tutorials*, vol. 20, no. 3, pp. 2429-2453, 2018.
- [6] N. Finn, "Introduction to time-sensitive networking," *IEEE Communications Standards Magazine*, vol. 2, no. 2, pp. 22-28, 2018.
- [7] G. P. Liu, et al, "Networked predictive control of systems with random network delays in both forward and feedback channels," *IEEE Transactions on Industrial Electronics*, vol. 54, no. 3, pp. 1282-1297, 2007.
- [8] D. Sun, et al, "Application of wave-variable control to bilateral teleoperation systems: A survey," *Annual Reviews in Control*, vol. 38, no. 1, pp. 12-31, 2014.
- [9] M. Matausek, et al, "A modified smith predictor for controlling a process with an integrator and long dead-time," *IEEE Transactions on Automatic Control*, vol. 41, no. 8, pp. 1199-1203, 1996.
- [10] N. Wang, et al, "Co-design of scheduling and control for networked control systems with time-delay and communication constraints," in *Proceedings of International Conference on Intelligent Human-Machine Systems and Cybernetics*, vol. 2, pp. 256-259, 2015.
- [11] P. L. Tang, et al, "Compensation for transmission delays in an ethernet-based control network using variable-horizon predictive control," *IEEE Transactions on Control Systems Technology*, vol. 14, no. 4, pp. 707-718, 2006.
- [12] T. Neagoe, et al, "NTP versus PTP in computer networks clock synchronization," in *Proceedings of IEEE International Symposium on Industrial Electronics*, vol. 1, pp. 317-362, 2006.
- [13] X. Tang, et al, "Output feedback predictive control of interval type-2 T-S fuzzy systems with Markovian packet loss," *IEEE Transactions on Fuzzy Systems*, vol. 26, no. 4, pp. 2450-2459, 2017.
- [14] Z. Wang, et al, "Stability analysis of event-triggered networked control systems with time-varying delay and packet loss," *Journal of Systems Science and Complexity*, vol. 34, no. 1, pp. 265-280, 2021.
- [15] D. W. Clarke, et al, "Generalized predictive control—part I. the basic algorithm," *Automatica*, vol. 23, no. 2, pp. 137-148, 1987.